# First Results from new SPIROC2E_ASIC

Urda Gómez, Lourdes

September 6, 2016

**Resumen**

The FLC group is a member of AHCAL group of DESY which belongs to the CALICE collaboration with others many internationl partners. One of the others partners is the OMEGA Group which deals in particular with the design of micro-electronic chips to equip several electromagnetic and hadronic calorimeter prototypes.

I participated in the FLC group as a summer student in the study of the front-end electronics of calorimeters. In particular, I worked with the electronic chip, called SPIROC2E, dedicated to the analogue hadronic calorimeter.

I have performed several measurements to study the reponse of the chip and carry out the chip characterization. The understanding of the reponse of these chips is an important step before equipping detectors for test beam measurements. In addition, these studies have provided a better understanding on the chip and have highlighted its limitations that should be improved in the next generation.

# Contents

# 1 Introduction and motivation

The ILC (International Linear Collider) is a project for a future linear collider in Japan. The ILC has the support of a huge collaboration that includes institutes and universities from countries from all the continents of the world. It collides electrons $e^-$ and positrons $e^+$, up to $1\,TeV$ energy in the center of mass and it will allow unprecedented high-precision measurements in the electroweak sector: top-quark physics, $W^-$, $Z^-$ bosons and the recently discovered in 2012 by the LHC experiment Higgs Boson. The ILC will allow to measure the Higgs boson couplings and properties at accuracies that are unreachable by LHC. It will provide a deep (and unfordable by other current experiments) understanding of the electroweak symmetry breaking mechanism. This will allow to test the robustness of the Standard Model of particles and other Beyond Standard Models at levels of precision never reached before.
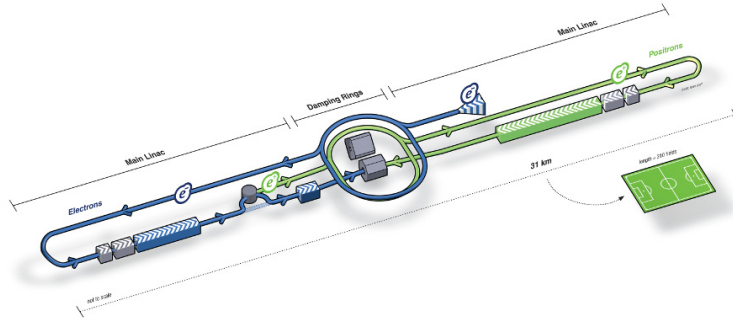


Figure 1: ILC design

The ILD (Internationnal Linear Detector) is a research project for a particles detector. This detector will be composed of sub-detector installed in concentric layers: a tracker to reconstruct the charged particle path, electromagnetic calorimeter (ECAL) and hadronic (HCAL), and a detector of muons. Each sub-detector has a particular role that allows to obtain information about the particles which pass through it. Calorimeters may use different technologies for measurements. Several projects are underway to evaluate the performance and the cost of these technologies.

The challenge is specially strong in the calorimetry since we would need to measure the energy with precision enough for resolving. This is not possible with "standard" calorimetry, so we need the Particle Flow.

The Particle Flow concept is based in the observation that most particles in a jet (charged particles and photons) can in principle be measured with much better precision than generally provided by the calorimeter for hadrons: charged particles energies are best measured with tracking systems, which offer relative resolutions of about $10^{-4}E(GeV)$, and individual photon energies can be measured with relative precision of about $15\,\%/\sqrt{E(GeV)}$ or better in electromagnetic calorimeters [4]. For this, Particle Flow requires high granularity calorimeters with minimum amounts of dead material that it does not allow to have active cooling systems (Power Pulsing). This also means that is required to concentrate the electronics and data processing already inside the detector, front-end electronics: reduction of cables, managment of millions of channels, etc.

One of the solutions, for the hadronic calorimeter is the AHCAL. In particle, physics calorimeters are used to determine the energy of particles by absorbing them in matter. To measure the energy transferred from the particle to the material, a signal proportional to the energy loss has to be extracted somehow. The effective energy resolution of a real calorimeter is limited, for example because only a fraction of the total deposited energy is measured. With a highly granular calorimeter it is also possible to identify local energy depositions from electromagnetic subshowers for selective energy dependent reweighting: this is called Software Compensation and will not be discussed in detail in this report.

The AHCAL physics prototype is a sandwich calorimeter consisting of 48 layers of steel absorbers. One cell structure had been designed alternating layers of absorbent materials (Tungsten or Steel) and Scintillator as active material (scintillating emitting materials produce photons in the range of the photomultiplier) to obtain a good energy resolution. This active layers are segmented into scintillator tiles, and each tile is read out by an individual silicon photomultiplier (SiPM).

AHCAL will use SiPM (Silicon photomultiplier) connected to a microchip (SPIROC). The SiPM uses the photoelectric effect: a photon hits a silicon atom and pulls an electron. Then this is multiplied by a photodiode:

it can be possible with the application of a high voltage. The SiPM was chosen because it has a High Gain. It is insensitive to magnetic fields and it has a good resolution for count photons.

To collect data, a frontal electronic system is composed of associated photomultipliers with electronic chips or ASICs (Application Specific Integrated Circuits). They are placed on electronic cards embedded in the layer structure. In addition, an acquisition system (DAQ) brings together data from different layers. This system is important to compile data from over 8 million of channels in the barrel.

This report is focused in the characterization of the SPIROC2E microchip which is located in the layers, and what are its optimal parameters of functioning.

# 2 SPIROC2E Chip

The CALICE collaboration has designed an analogue HCAL prototype using Scintillating fibers read out by SiPM detectors. A new front-end chip called SPIROC (standing for Silicon PM Integrated Read Out Chip) has been designed to read out the upcoming technological demonstrator. Currently the second generation (SPIROC2) has been delivered. It corrects the bugs observed of the first version SPIROC1.

One major advantage of the front-end electronics is that it can run in power pulsing mode. The power pulsing will save huge amount of energy. Each channel should not consume more than $25\,\mu W$ per passing beam (a processor of a portable computer consumes $20\,W$ when it idles).

Digitization is inside of SPIROC and this chip is dedicated very front-end electronics for an ILC prototype hadronic calorimeter with SiPM readout. It has been realized in $0.35\,\mu m$ SiGe technology. It has been developed to match the requirements of large dynamic range, low noise, low consumption, high precision and large number of readout channels needed. It is an auto-triggered, bi-gain, 36-channel ASIC which allows to measure on each channel the charge from one photoelectron to 2000 and the time with a $100\,ps$ accurate TDC. An analog memory array with a depth of 16 for each is used to store the time information and the charge measurement. A 12-bit Wilkinson ADC has been embedded to digitize the analog memory contents (time and charge on 2 gains). The data are then stored in a $4\,kbytes$ RAM. A very complex digital part has been integrated to manage all theses features and to transfer the data to the DAQ.

## 2.1 Presentation of the SPIROC2E's electronic

The analogue core is composed of 36 channels embedding an input DAC for SiPM high voltage adjustment on $5\,V$ to tune gain channel by channel. Two preamplifiers alllow the requested dynamic range and are followed by a trigger line made of a fast shaper and a discriminator. The charge measurement line is made of two variable slow shapers. The block scheme of a channel for the SPIROC2 is shown on the next figure.
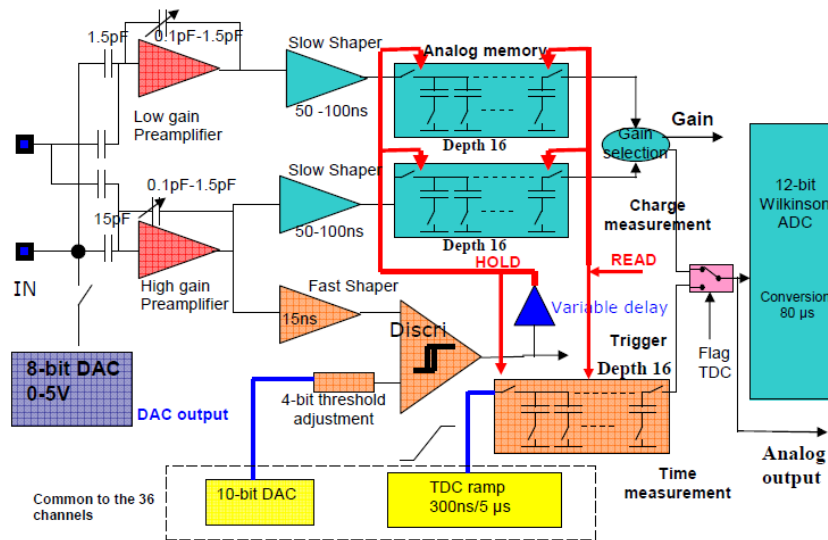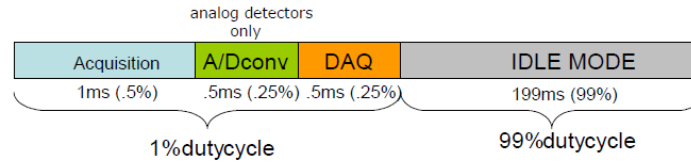


Figure 2: SPIROC2 Analog Part

The ADC used in SPIROC is based on a Wilkinson structure. Its resolution is 12 bits. As the default accuracy of 12 bits is not always needed, the number of bits of the counter can be adjusted from 8 to 12 bits.

This type of ADC is particularly adapted to this application which needs a common analogue voltage ramp for the 36 channels and one discriminator for each channel. The ADC is able to convert 36 analogue values (charge or time) in one run (about $100\,\mu s$ at $40\,MHz$) [2].

### 2.1.1 SPIROC Digital Part

The system on chip has been designed to match the ILC beam structure. The complete readout process needs at least 4 different steps: acquisition phase, conversion phase, readout phase and possibly idle phase [2].



*Digital part phases versus time.*

| Acquisition | A/D conversion | DAQ |
|---|---|---|
| When an event occurs :<br>• Charge is stored in analogue memory<br>• Time is stored in digital (coarse) and analogue (fine) memory<br>• Trigger is automatically rearmed at next coarse time flag (bunch crossing ID)<br><br>Depth of memory is 16 | The data (charge and time) stored in the analogue memory are sequentially converted into digital data and stored in a SRAM. | The events stored in the RAM are readout through a serial link when the chip gets the token allowing the data transmission.<br>When the transmission is done, the token is transferred to the next chip.<br>256 chips can be read out through one serial link |

Figure 3: SPIROC Digital Part Diagram

### 2.1.2 Link between DAQ and SPIROC

This 3 modules of the digitals parts are activated by signals form the DAQ. These signals are given below.
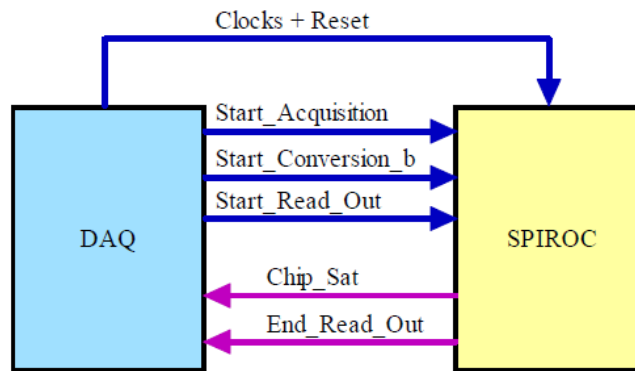


*Main Signals between DAQ and SPIROC*

Figure 4: Link between DAQ and SPIROC

The rising edge of the Start_Acquisition signal is the beginning of the acquisition phase for the digital part. The end of the acquisition is given by the falling edge of this signal [2].
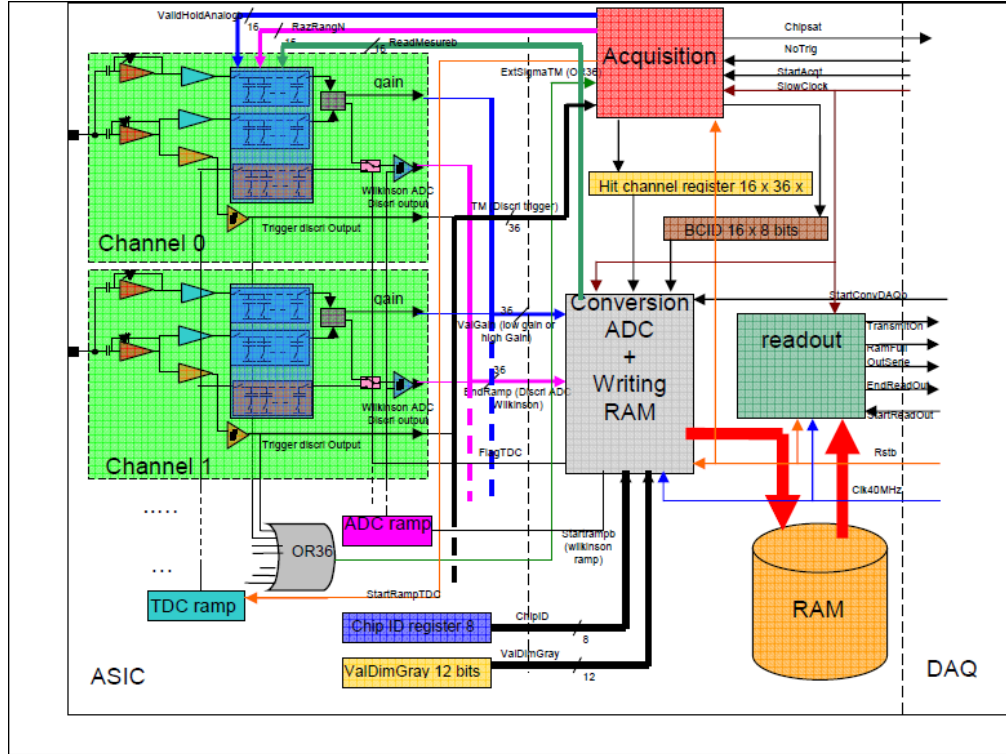
## 2.2 General operation



Figure 5: General operation diagram

## 2.3 External and Auto Trigger modes

When we work with an operating detector we need a trigger system because only a few events are physically measurable. The triggerest is an essential part of a detector , indeed it selects certain events considered important. It triggers the reading of a signal by the front-end electronics and together with its registration. SPIROC2E can run in fully Auto Triggered mode and alse External Triggers [4]. Additionally and external validate can be used in combination with the Auto Trigger, so that only events that are coincident with an External Trigger are saved:

- **Auto Trigger:** The global trigger threshold can be configured for the whole chip via a $10\,bits$ register with $4\,bits$ of fine tuning per channel. Chips readout the information if a channel gets signal over certain threshold. This first triggered channel in a given cycle triggers sampling of all 36 channels.Channels triggering after the first in the same cycle are lost.

- **External Trigger:** The chip is forced after a fixed amount of time (trigger distance). An External Trigger signal can also be fed directly into SPIROC2E. For an externally triggered event all "flags" are set. Owever, even in External Trigger mode, the Auto Trigger can not be disabled completely. Even for the highest possible global threshold some channels will fire the Auto Trigger. External trigger is for debugging and LED calibration only because there will be no External Trigger in ILC and in testbeam trigger will arrive to late at SPIROCS.

## 2.4 High Gain and Low Gain configuration

The high-gain mode is used for small signals and calibration up to 100 fired pixels, corresponding to around 6 MIPs. Low-gain mode has a fixed $\sim 1:10$ (we need to calibrate it) ratio compared to high-gain mode, extending the dynamic range up into SiPM saturation. The signals for both modes are generated in parallel from two separate charge preamplifiers with switchable feedback capacities for gain adjustment. Feedback capacities can be configured in a 6 bit register from $25\,fF$ to $1575\,fF$.

To take measurements SPIROC can work in two modes: HG/LG and ADC/TDC. The first one ignores TDC information and it provides ADC/LG and ADC/HG information. The second one keep ADC and TDC but add a new bit (0/1) that tell us if the data was taken in HG or LG.

## 2.5   LED calibration system

To carry out the calibration of the system we use LED and charge injection. The LED calibration system is integrated in the HBU and it consists of 1 UV LED per channel that irradiates a selectable amount of light into each scintillator tile.

Using the LED system, tests of the full HBU signal chain from the scintillator tile through signal sampling and digitisation can be performed. This is primarily used to judge the performance of SiPM gain calibration, but also for different calibration tasks. In addition, the LED system test stand is used to determine LED pulse quality of each individual channel. All measurements are performed on the same HBU in High Gain mode [5].

# 3   SPIROC2E Chip Characterization

SPIROC inputs consists of different stages and each one has its role in the chip. A pre-amplifier for amplifying the input signal, the slow shaper allows to shape the signal. The ramp allows the conversion of the analog signal of Voltage into ADC unit, the fast shaper that can give the trigger signal and a delay box that delays the trigger signal end of measuring the maximum signal [3].

To do tests on SPIROC, a test bench was set up. It consists of a circuit board with ASIC and a FPGA (this could be programmable) controlled by a data acquisition interface: Labview software. The FPGA transfers the data to a computer via USB. The input signal was from a generator.

## 3.1   Experimental set up and procedure

For the experimental set up we count on a pulse generator to do the first measurements and a LED calibration system for gain and pedestal stability measurements. In addition to carry out the data acquisition phase, we have a LabView interface to adjust the best paramaters to take data.
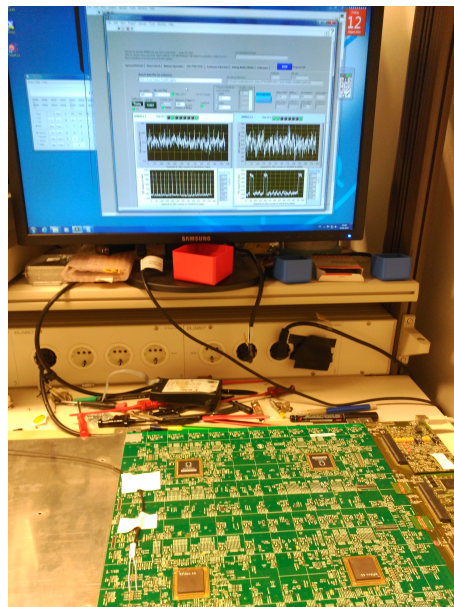


Figure 6: Set up and LabView Interface

The HBU consist of four SPIROC with 36 channels per chip. Note that we only had been working with one SPIROC2E located in the second quadrant. In Figure 6 we can appreciated the electronic of the system wich is connected to computer (LabView) by a USB conection.
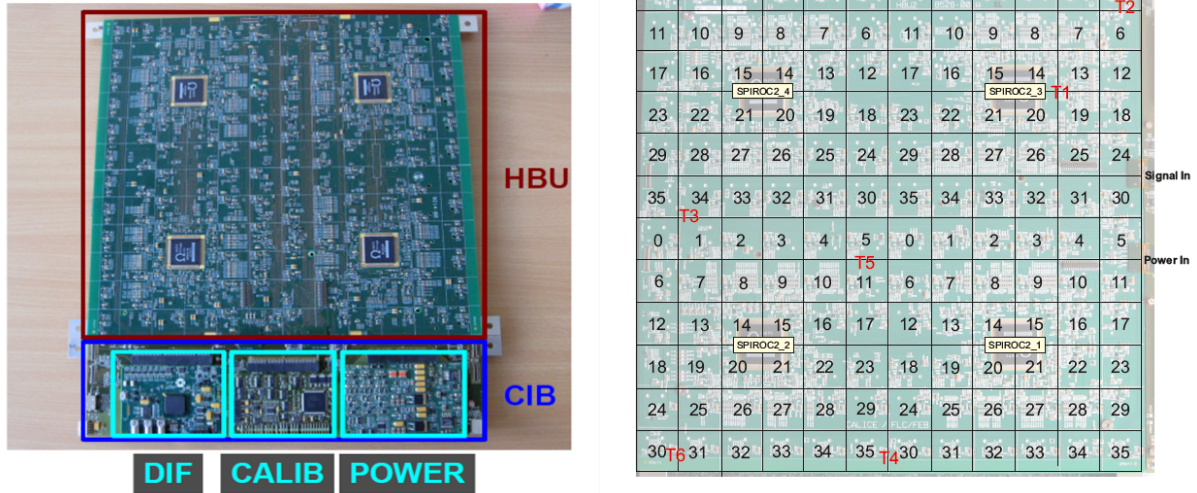
Figure 7: HBU2 tile map (top view).

Notice that in Figure 7 is SPIROC2E_2 instead of SPIROC2_2 [2].

## 3.2 Measurements taken with the pulse generator

### 3.2.1 Holdscan

The hold time is the minimum amount of time the data input should be held steady after a clock event, so that the data is reliably sampled by a clock. The "Délai" (Figure 8) is the time between which the trigger is done and measurement signal [1]. It should fit snugly to measure the maximum signal, as this helps to separate the noise from the signal. In addition, delay variation is then used to reconstruct signal point by point output of the shaper slow. To carry out the measurements related to holdscan we connected the board (with all the electronic) to a voltage source ($\sim 6\,V$) during $100\,cycles$ and a fixed shapping time. We were varying the value of the preamplifier from $100\,fF$ to $400\,fF$ (to $625\,fF$ in External Trigger mode case) and we obtain the next results for holdtime to external and Auto Trigger mode respectively. Notice that the holdtime value corresponds with the largest amplitude in the signal in each case.
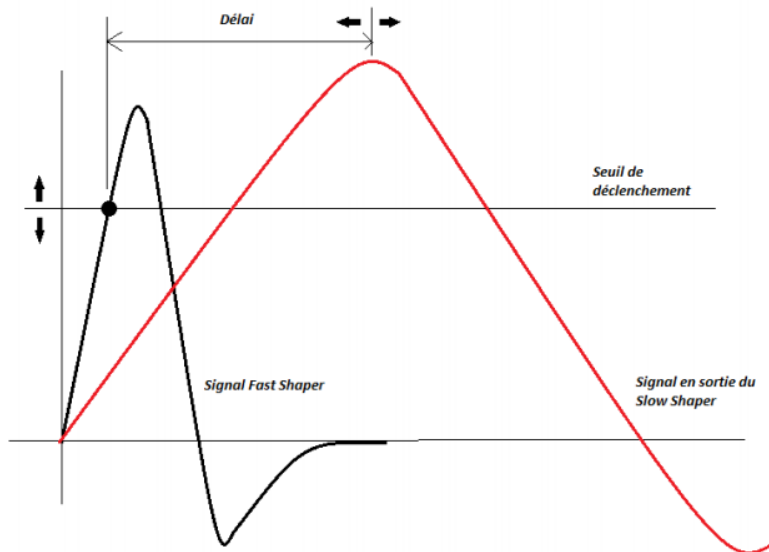


Figure 8: Holdtime diagram

First, we took measurement of amplitude in ADC units. We were changing the value of the shaping time in HG and LG modes with a fixed value for the preamplifier. The results are shown in the next plot:
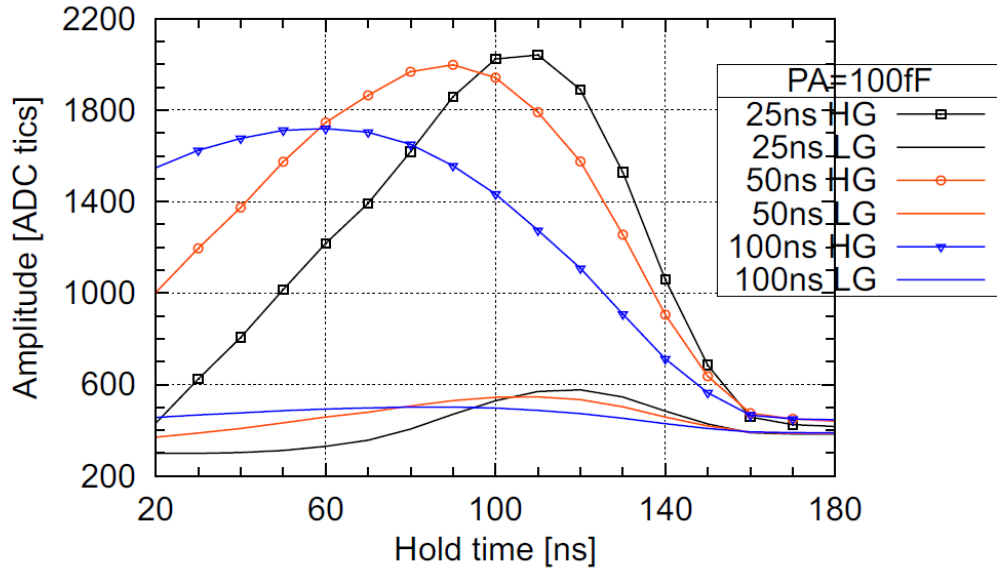


Figure 9: Holdtime for differents shaping time

From Figure 6 we can conclude that the best shaping time to take the data is $50\,ns$. It is because of the amplitude of the signal of the red graph is the most large and we can fit it with a good parameters.

For next study, shaping time is fixed a different preamplifier values are used. This is done for ET (Figure 10) and AT (Figure 11). We can see the value of the best holdtime for each value of preamplifier with just locating the maximums in X-axis.

**3.2.1.1   External Trigger mode**   The results for the External Trigger mode for High and Low Gain mode are shown in the next Figure:
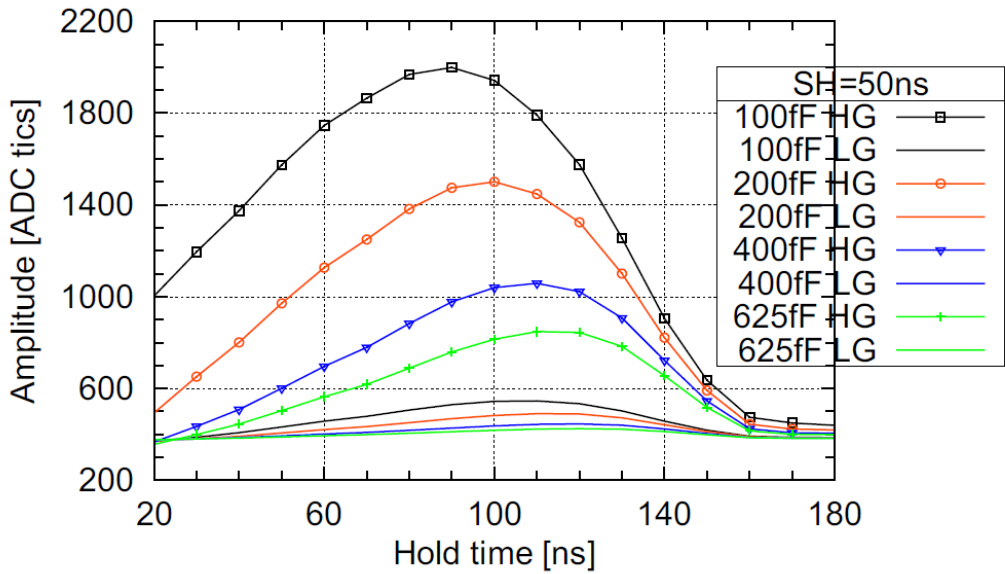


Figure 10: Holdtime for External Trigger mode

**3.2.1.2  Auto Trigger mode**  The results for the Auto Trigger mode for High and Low Gain mode are shown in the next Figure:
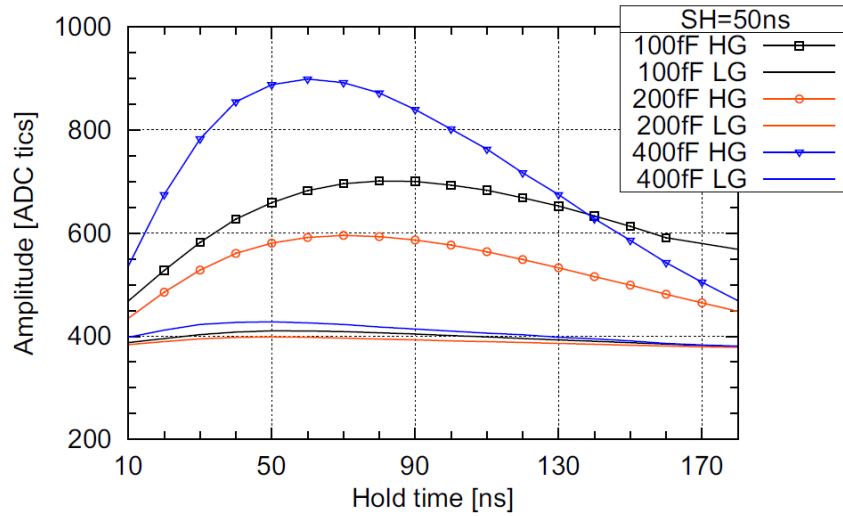


Figure 11: Holdtime for AutoTrigger mode

We obtain a shorter optimal hold value as expected.

### 3.2.2  Dynamic Range

Dynamic range is the ratio between the largest and smallest values that a certain quantity, such as in signals like sound and light, can assume. In particular, it is the signal range we have and that we measure in ADC units. In addition, it is different for HG and LG modes. To measure it, the chip was again connected to the pulse generator with an increasing amplitude and with a fixed shaping time ($sh = 50\,ns$). We were varying the value of the preamplifier from $100\,fF$ to $400\,fF$ (except $300\,fF$) in $100\,fF$ steps and we were mostly interesting in High Gain because we can see when the chip is saturated: we can check that the saturation charge is slower with a higher value of preamplifier. Next plots show us the measurements to external and Auto Trigger mode respectively:

**3.2.2.1  External Trigger mode**  The results for the External Trigger mode for high and Low Gain mode are shown in the next Figure:
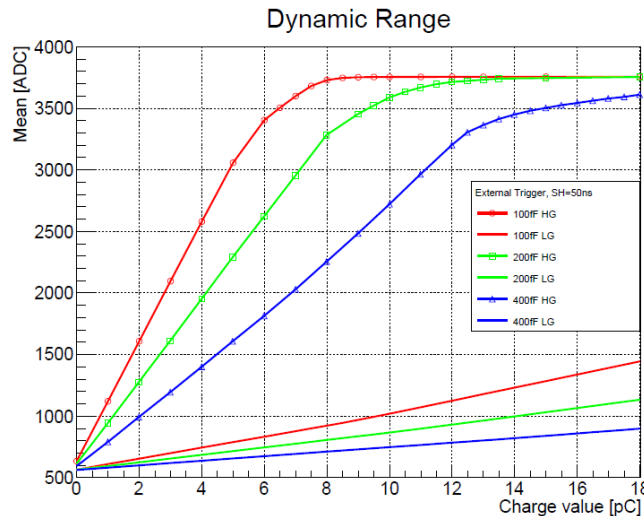


Figure 12: Dynamic range for External Trigger mode

**3.2.2.2 Auto Trigger mode** The results for the Auto Trigger mode for high and Low Gain mode are shown in the next Figure:
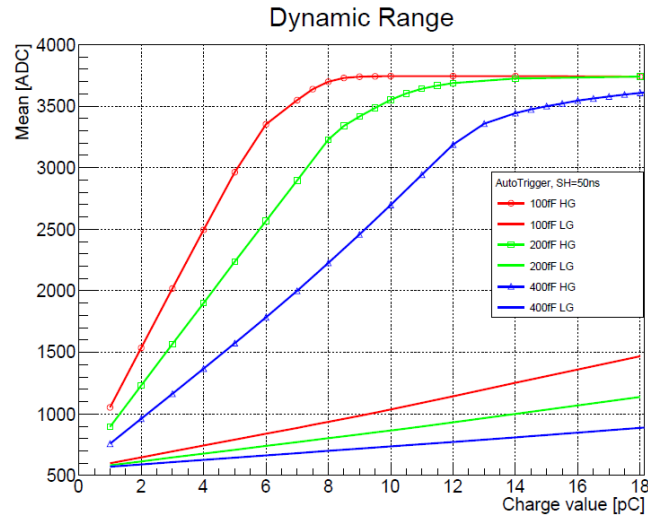


Figure 13: Dynamic Range for AutoTrigger mode

Notice that we had to take more data when the value of the charge is near to saturation to obtain more estadistic.

What is more, if we represent the amplitude AT (Auto Trigger) vs amplitude ET (External Trigger) we obtain a linear fit as expected:
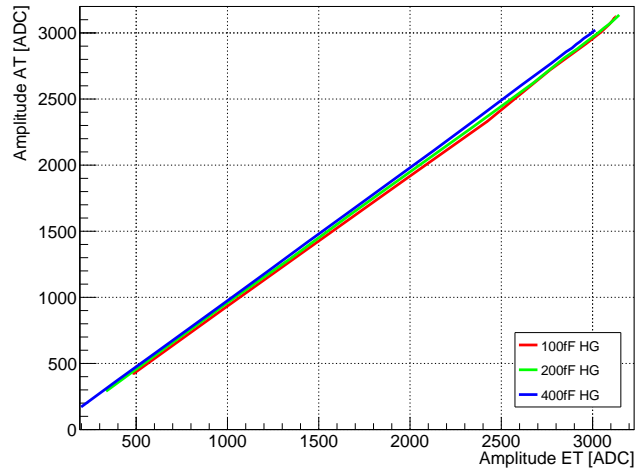


Figure 14: Amplitude AutoTrigger vs Amplitude External Trigger

### 3.2.3 Intercalibration

This part is use to determine, check, or rectify the graduation of the instrument giving quantitative measurements. In particular, we know that the relation between High Gain and Low Gain is around 1 : 10 but we need to know this intercalibration factor exactly to do testbeam for instance. Intercalibration uses the results from dynamic range measurements we use again pulse generator and a holdtime fixed in $100\,ns$:

**3.2.3.1 External Trigger mode** The results for the External Trigger mode are shown in the next Figure:
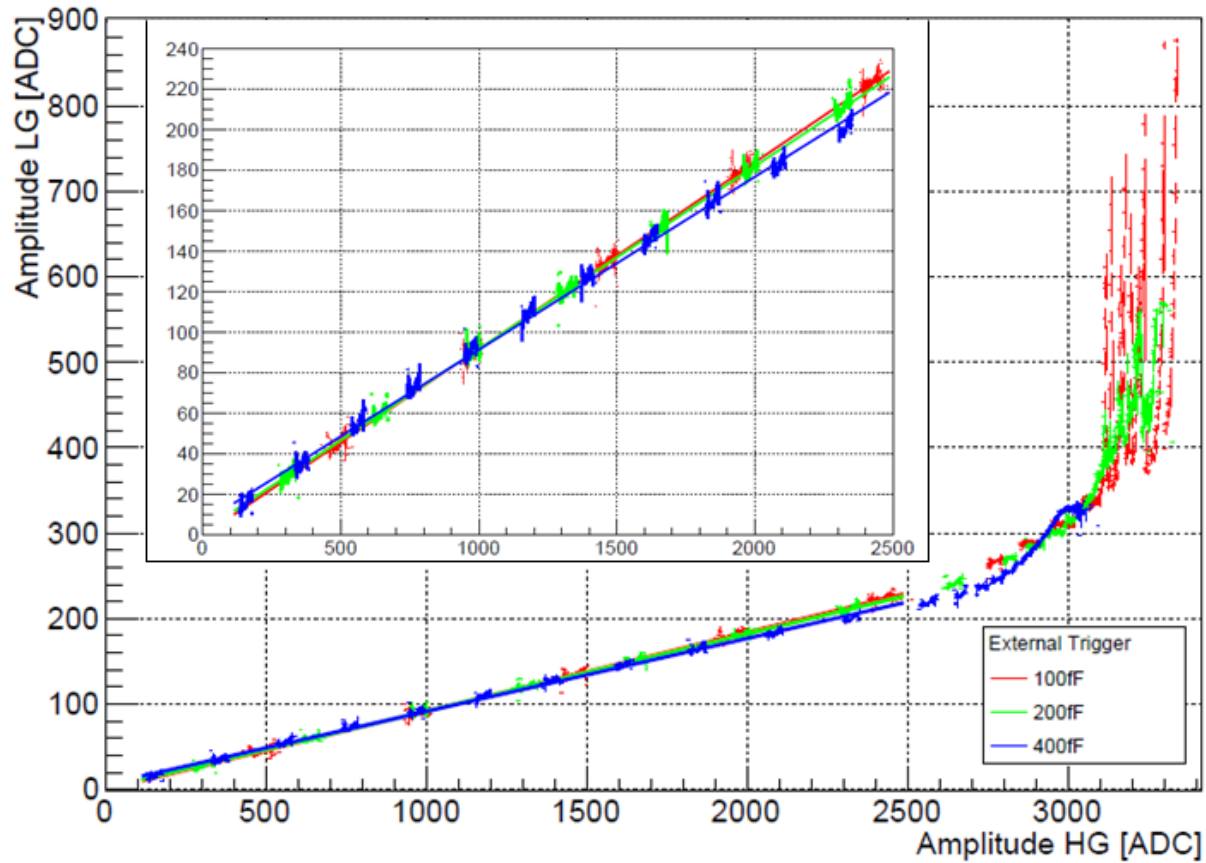


Figure 15: Intercalibration for External Trigger mode

If we fit the date for each value of preamplifier with a linear fit $y = p_0 + p_1 x$ we obtain the next parameter for the External Trigger mode:

| $PA\,(fF)$ | $p_0\,(ADC)$ | $p_1$ |
|---|---|---|
| 100 | $0.04 \pm 015$ | $0.09177 \pm 0.00009$ |
| 200 | $1.51 \pm 0.12$ | $0.09021 \pm 0.00008$ |
| 400 | $6.11 \pm 0.09$ | $0.08532 \pm 0.00006$ |

Table 1: Adjustment parameters

The value of $p_1$ corresponds to the intercalibration factor.

**3.2.3.2 AutoTrigger mode** The results for the External Trigger mode are shown in the next Figure:
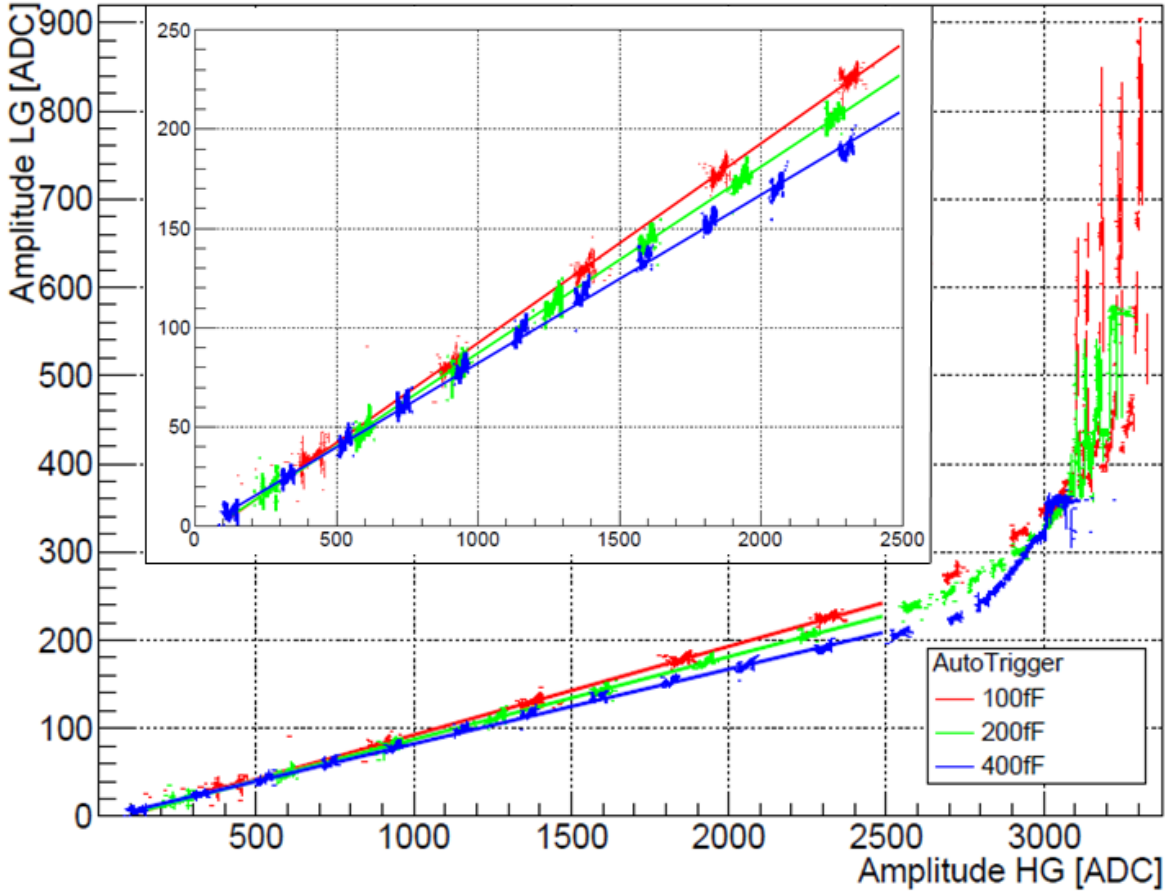


Figure 16: Intercalibration for AutoTrigger mode

If we fit the date for each value of preamplifier with a linear fit $y = p_0 + p_1 x$ we obtain the next parameter for the Auto Trigger mode:

| $PA\,(fF)$ | $p_0\,(ADC)$ | $p_1$ |
|---|---|---|
| 100 | $-8.08 \pm 0.12$ | $0.10052 \pm 0.00010$ |
| 200 | $-6.38 \pm 0.12$ | $0.09394 \pm 0.00010$ |
| 400 | $-2.37 \pm 0.09$ | $0.08480 \pm 0.00007$ |

Table 2: Adjustment parameters

The value of $p_1$ corresponds to the intercalibration factor.

## 3.3 Measurements with LED calibration system

The following measurements have been done using the LED calibration system insted of the pulse generator. In our case, the channels wich were equipped with scintillator material are: 3, 5, 6, 8, 17, 21, 23 and 31 (In SPIROC2E_2 in Figure 7).

### 3.3.1 Gain

Because of large individual variations in gain, optimal bias voltage and response to environmental factors (especially the temperature), the gain factor of each SiPM in the AHCAL has to be monitored constantly to ultimately determine the amount of energy deposited per tile. As each pixel should emit the same charge upon being hit, the

charge spectrum of a SiPM illuminated by short (∼ns), low-amplitude (2-4 average photon hits) flashes of light exhibits a quantisation of detected charges. This results in a spectrum composed of single peaks. The first of these peaks represents the pedestal, the readout value for no signal, while the others are pixel peaks. Such single photon spectra (SPS) can be fitted, for example with a sum of single Gaussian distributions. From the distance between these peaks the SiPM gain can be extracted in arbitrary digitisation units. Together with the pedestal position, these can be utilised to convert measurements to the pixel scale. The pixel scale is a normalised measure of the detected light amplitude [4].

Gain calibration is done by flashing small amplitude light pulses into each scintillator tile mounted on the HBU. During operation the light amplitude can be controlled by setting the VCalib DAC in the DAQ software. The time between pulses can also be configured.

Now, we use LED light and we run it in External Trigger mode and we took measurements of channels with scintillator material. The resulting plots and the table with the values of gain are the next:

| $Channel$ | $Gain\,(ADC)$ |
|-----------|---------------|
| 3 | $46.7 \pm 0.3$ |
| 5 | $40.9 \pm 0.8$ |
| 6 | $46.8 \pm 1.6$ |
| 8 | $43.564 \pm 0.006$ |
| 17 | $46.3 \pm 0.5$ |
| 21 | $46.5 \pm 0.3$ |
| 23 | $41.6 \pm 0.8$ |

Table 3: Gain values for the channels with scintillator material

Notice that the channel number 31 does not appear because it was damaged for some reason and its results are not reliable.

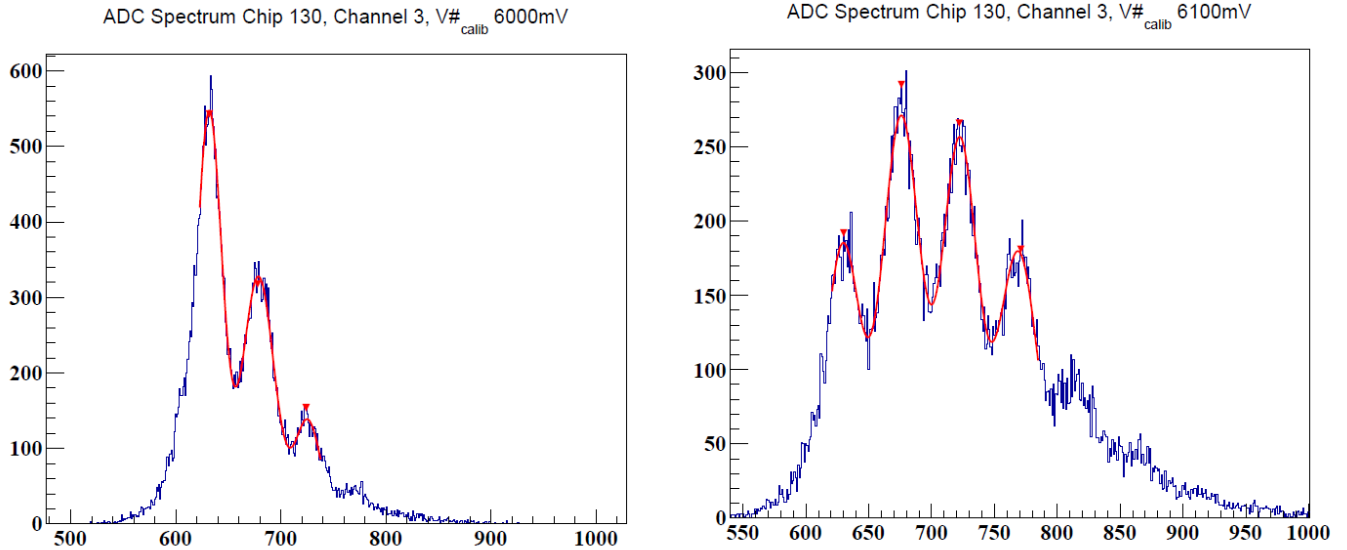The fits for the channels without scintillator material for differents values of voltage are the next:



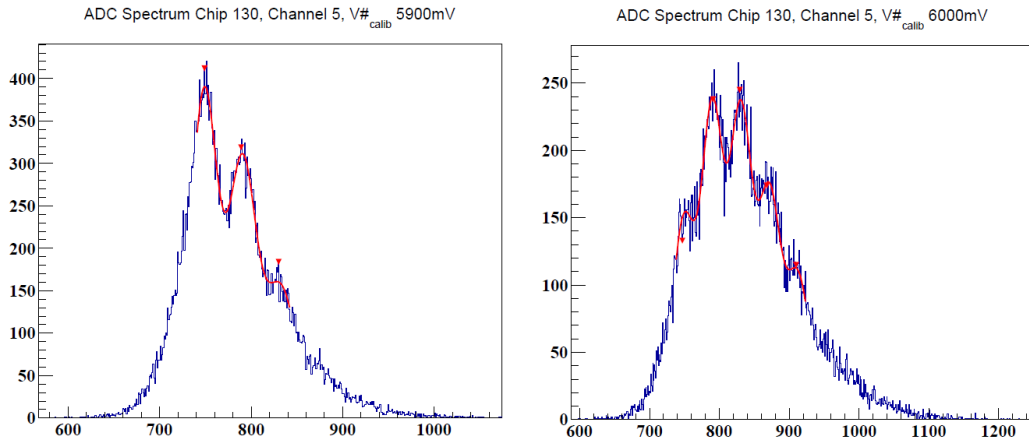Figure 17: ADC Spectrum, Chip 130, Channel 3 for $6000\,mV$ and $6100\,mV$

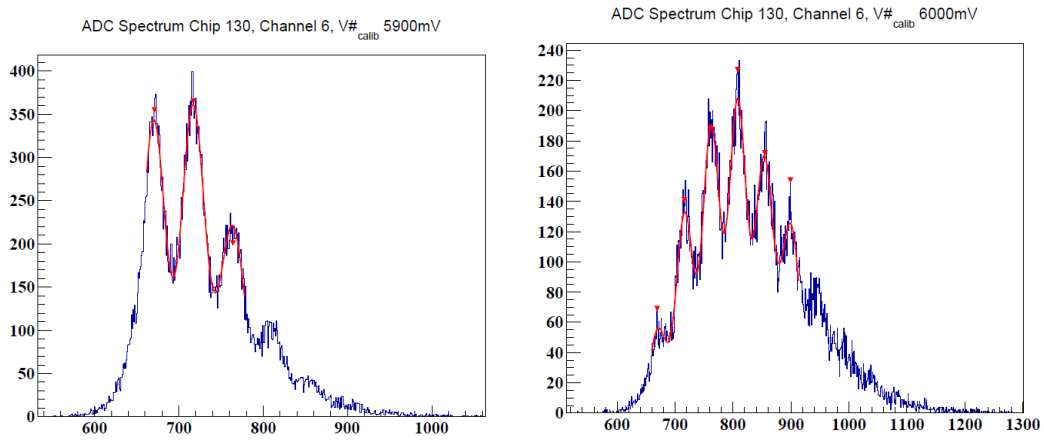Figure 18: ADC Spectrum, Chip 130, Channel 5 for $5900\,mV$ and $6000\,mV$

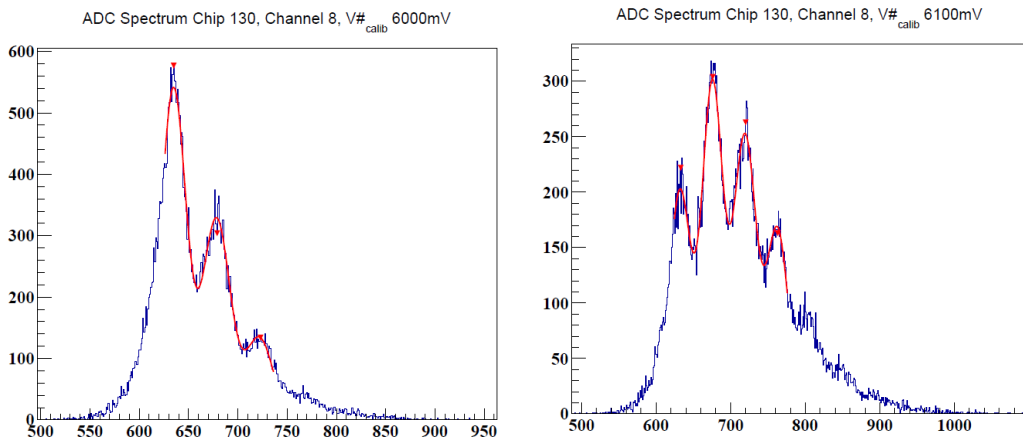Figure 19: ADC Spectrum, Chip 130, Channel 6 for $5900\,mV$ and $6000\,mV$

Figure 20: ADC Spectrum, Chip 130, Channel 8 for $6000\,mV$ and $6100\,mV$
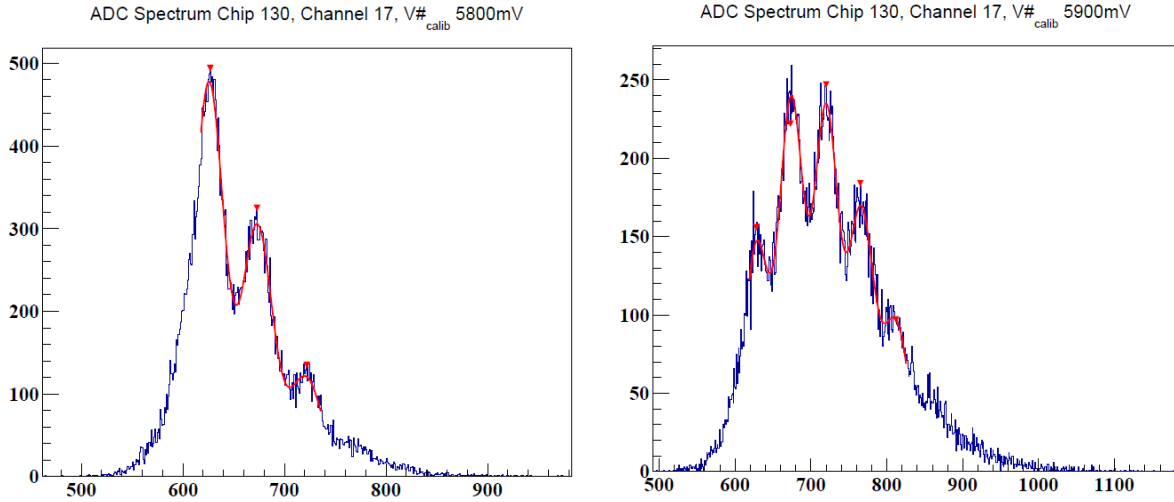
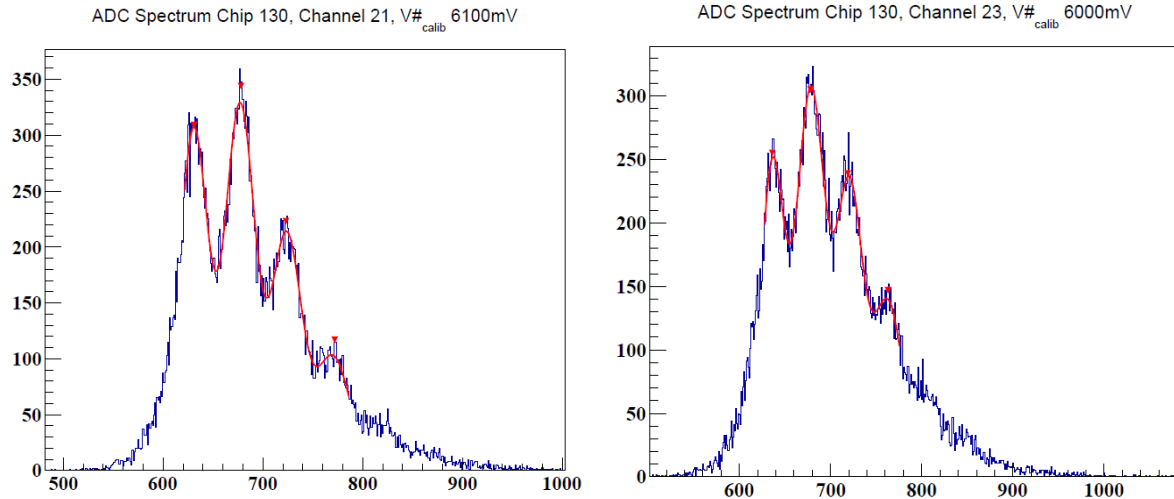Figure 21: ADC Spectrum, Chip 130, Channel 17 for $5800\,mV$ and $5900\,mV$



Figure 22: ADC Spectrum, Chip 130, Channel 21 and Channel 23 for $6100\,mV$ and $6000\,mV$ respectively

We have to notice that this fits are worse than the fits of SPIROC2B because of the noise. The noise causes wide peaks and it affects to the value of gain.

### 3.3.2 Pedestal shift

Any electronic device has a ground level, called pedestal. This ground level fluctuates, typically following Gaussian statistics around a mean value. The Pedestal signal is the convoluted effect of electronics and SiPM noise, in a given interval of time. The mean of the pedestal signal will be referred to as pedestal value, and its width is considered to be the noise [5].

Pedestal shift is an important issue on the second generation of SPIROC. It has been observed that the pedestal values depend on the total charge injected into the inputs of the chip. If several channels saturate at once, the pedestal level can even go into the negative ADC region, reading as zero. This poses a problem mainly for calibration measurements, as usually the pedestal shift expected for signals from typical test beam measurements [6] is only in the range of a few MIPs at once, which is low enough not to be a problem.

For calibration measurements several workarounds have to be used. It is possible to calibrate channels in several runs with only parts of the channel active at a time. Lowering trigger rates and possibly signal amplitudes also helps in reducing the effect.
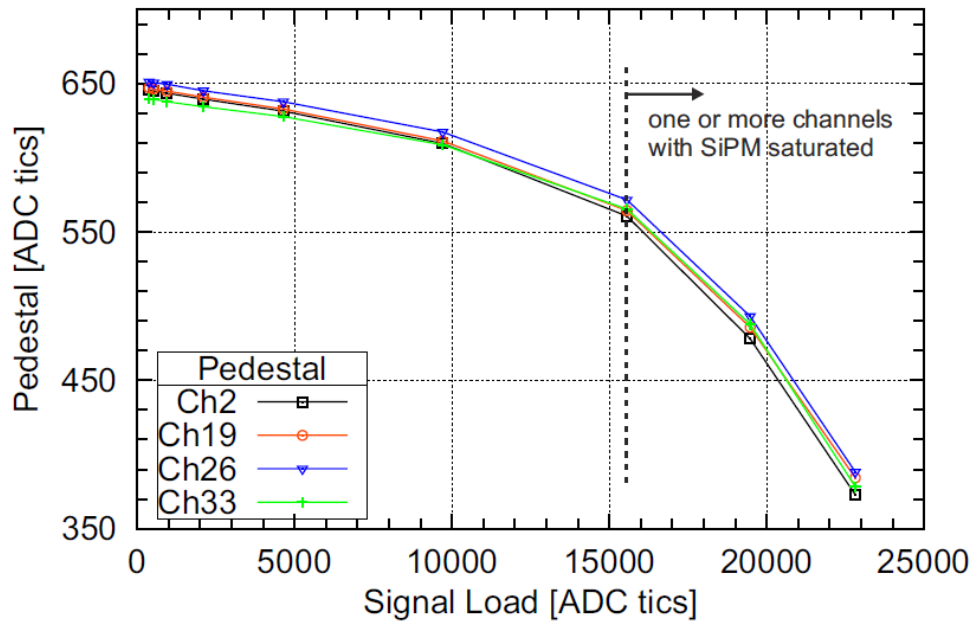


Figure 23: Pedestal Shift graph

The pedestal has been measured in all non-equipped channels and plotted as a function of the sum of mean of the ADC spectra of all equipped channels. This has been done for LED runs taken with several LED amplitudes. For large amplitudes, the equipped channels start to saturated and then the pedestal shift of the others increases faster.

If we compare our results with other previos results from SPIROC2D and SPIROC2B we can conclude that in this respect, SPIROC2E and SPIROC2D are much better than SPIROC2B. The last one has a linear performance in front the performance of the others two.
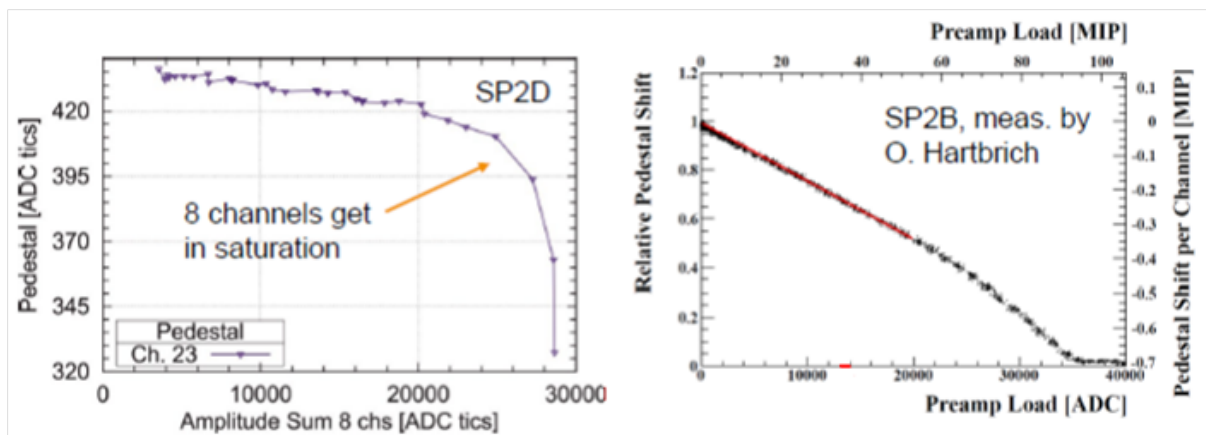


Figure 24: Previous results

# 4 Conclusion and outlook

- Short overview to the physics motivations with the project of the future the International Linear Collider. It promise an unprecedented high-precision measurements in the high energy physics using the concept of Particle Flow which requires very high granularity calorimeters.

- The AHCAL detector is one of the approaches: it is now in the engineering prototyping phase, lead by DESY FLC group.

- This satisfactories results may be used to perform a successfully characterization of the chip SPIROC2E about its holdtime, dynamic range, intercalibration factor between High Gain and Low Gain mode and the LED calibration system for gain and pedestal shift.

- This chip has been specially designed to test the Power Pulsing but it is out of this study.

- TDC characterization has to be done: we only have done the ADC characterization in this report.

# References

[1] EldwanBrianne. *Caractérisation de l'électronique frontale d'un calorimètre à hautegranularité.*

[2] SPIROC 2 User Guide (Draft).

[3] EldwanBrianne. *Studies of the front-end electronics of the Analog HCAL.*

[4] Master-Thesis by Oskar Hartbrich. *Commissioning and LED System Tests of the Engineering Prototype of the Analog Hadronic Calorimeter of the CALICE Collaboration.*

[5] Sarah Schröder. *Commissioning of a prototype hadronic calorimeter*

[6] http://flcwiki.desy.de/